DYNAMIC APERTURE STUDY FOR THE NLC MAIN DAMPING RINGS*

A.Wolski#, M.Venturini, S. Marks, LBNL, Berkeley, California 94720, USA

Abstract

A sufficiently large acceptance is critical for the NLC Main Damping Rings (MDR) as the high power carried by the beams demands very high injection efficiency. Chromatic sextupoles and wiggler insertions (needed for rapid damping) are substantial sources of nonlinearities limiting the dynamic aperture. We report on the techniques we are using for analysis of single-particle beam dynamics in the presence of wiggler fields with significant nonlinear components. We demonstrate that our approach gives results in good agreement with experimental data when applied to the BL11 wiggler in SPEAR2, and discuss the present status of studies for the NLC MDR.

INTRODUCTION

The Main Damping Rings [1] of the NLC are designed to reduce the incoming normalized beam emittances from 150 μm to 3 μm horizontally and 0.02 μm vertically, in a time consistent with the machine repetition rate of 120 Hz. The short damping times needed (around 5 ms) are achieved in a 300 m lattice by use of over 60 m of wiggler with peak field 2.1 T. The wiggler provides 90% of the synchrotron radiation energy loss in the ring. The high average injected beam power of 60 kW means that injection efficiency close to 100% must be achieved to avoid radiation damage to components of the ring; large physical and dynamic apertures are therefore needed.

Experience at SPEAR2 of a wiggler that led to a significant reduction in dynamic aperture [2] motivated detailed studies for the NLC MDR. Studies one year ago [3] identified a large dynamic octupole component in the MDR wiggler, arising from the interaction between the trajectory in the wiggler and the fourth-order roll-off of the vertical field with horizontal position. This leads to a large tune-shift with betatron amplitude for particles in the ring, and limits the dynamic aperture.

Recently, a more detailed analysis of the field data from the magnetic modeling code used to design the MDR wiggler revealed limitations on the numerical quality of the field data. In particular, significant deviations from the constraints imposed by Maxwell's equations were found close to the pole faces. New field data have therefore been produced, with tighter limits on the numerical quality, and this has led to a significantly revised estimate on the size of the dynamic octupole component. This experience has emphasized for us the importance of field data of very high quality for calculating the beam dynamics in the field of a device such as a wiggler.

*Work supported by the US DOE under contract DE-AC03-76SF00098
#awolski@lbl.gov

We have also extended the techniques we are using to study the beam dynamics to include use of differential algebra (DA) tools for producing a higher-order dynamical map for a periodic section of the wiggler. Previous studies were based on dynamical maps limited to third order.

In this paper, we first describe the techniques that we have developed for producing a dynamical map given a numerical magnetic field map for one periodic section of a wiggler. We use the SPEAR2 BL11 wiggler as an example, since we are able to validate our analysis against experimental data. We then apply the same techniques to the NLC MDR. The numerical quality of the field data for the MDR wiggler still appear not as good as the data for the SPEAR2 BL11 wiggler, and it is hoped to address this issue in the future. The results presented here for the beam dynamics in the MDR should therefore be regarded as preliminary.

FIELD FITTING

The first step in our analysis of beam dynamics in a wiggler is to fit the numerical field data with an analytic series. This will allow the generation of a dynamical map in Taylor form, using a differential algebra code. Appropriate expressions (satisfying Maxwell's equations) can be given in either cylindrical polar co-ordinates, or rectangular Cartesian co-ordinates. In cylindrical co-ordinates, the field components can be written:

$$\begin{aligned} B_\rho &= \sum_{mn} \alpha_{mn} \mathrm{I}'_m(nk_z\rho)\sin(m\phi)\cos(nk_z z) \\ B_\phi &= \sum_{mn} \alpha_{mn} \frac{m}{nk_z\rho} \mathrm{I}_m(nk_z\rho)\sin(m\phi)\cos(nk_z z) \\ B_z &= -\sum_{mn} \alpha_{mn} \mathrm{I}_m(nk_z\rho)\sin(m\phi)\sin(nk_z z) \end{aligned} \qquad (1)$$

In Cartesian co-ordinates the components are:

$$\begin{aligned} B_x &= -\sum_{m,n} c_{mn} \frac{mk_x}{k_{y,mn}} \sin(mk_x x)\cos(nk_z z)\sinh(k_{y,mn} y) \\ B_y &= \sum_{m,n} c_{mn} \cos(mk_x x)\cos(nk_z z)\cosh(k_{y,mn} y) \\ B_z &= -\sum_{m,n} c_{mn} \frac{nk_z}{k_{y,mn}} \cos(mk_x x)\sin(nk_z z)\sinh(k_{y,mn} y) \end{aligned} \qquad (2)$$

The cylindrical representation (1) reflects the periodicity in the azimuthal and longitudinal co-ordinates. In the Cartesian representation (2), there is an artificial periodicity in the horizontal co-ordinate; nonetheless, it is possible by using a small enough value for k_x to obtain a very good fit to the field in the region of interest for the beam dynamics. The Cartesian representation is more convenient for use in beam dynamics codes, including the differential algebra codes we shall use to produce the dynamical map.

In practice, we find the most robust fitting method is to identify the coefficients of the cylindrical fit, α_{mn}, by a two-dimensional Fourier analysis of the radial field component on the surface of a cylinder, and then calculate the coefficients c_{mn} of the Cartesian fit using the following relationship:

$$\alpha_{mn} = \frac{2(-1)^{\frac{m-1}{2}} m!}{(nk_z)^{m-1}} \sum_{m'} \left(\sum_{q=0}^{\frac{m-1}{2}} \frac{k_{y,m'n}^{m-2q-1} (m'k_x)^{2q}}{(2q)!(m-2q)!} \right) c_{m'n} \qquad (3)$$

The coefficients c_{mn} can be found directly by a Fourier analysis of the vertical field component on some plane of fixed y; however the implicit periodicity of the field imposes a lower limit on the value of $k_x = \pi/2x_{max}$, where x_{max} is the limit of the range of the numerical field data. By making a cylindrical fit, and then using (3) to calculate the c_{mn}, we can choose a smaller value of k_x and obtain a better fit over a wider range.

As an example, we consider the SPEAR2 BL11 wiggler. A model of this device is provided in the distribution of the magnet code RADIA [4], and we have used this model to generate a numerical field map for one periodic section of the wiggler. As an indication of the quality of the field data, Figure 1 shows the divergence and curl of the field, calculated from the field data, on a plane 6 mm above the mid-plane. The peak field is 2 T, and the period is 175 mm; the full-gap between the upper and lower poles is 16 mm. We observe some deviation from zero over a narrow longitudinal region close to the edge of the pole, where the vertical field is falling rapidly.

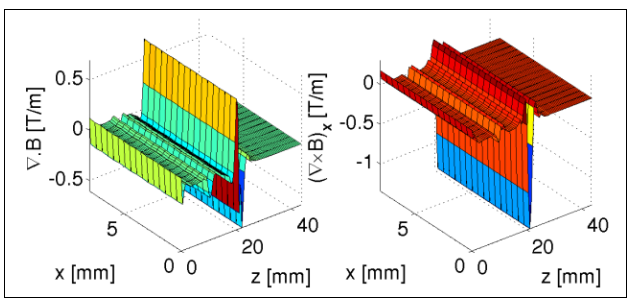

Figure 1: Field divergence and curl of the SPEAR2 BL11 wiggler field map, on a plane 6 mm above the mid-plane.

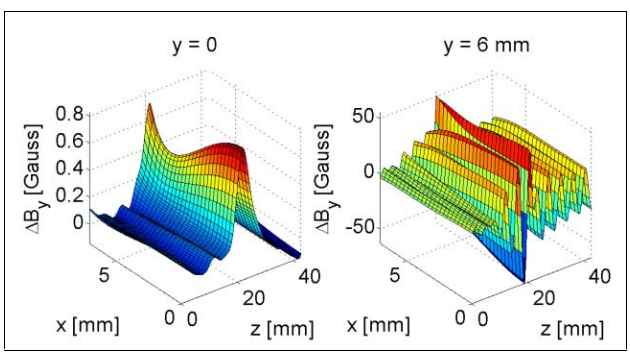

Figure 2: Residual of a fit to the SPEAR2 BL11 wiggler field map.

We fitted the field by first calculating the cylindrical coefficients using a Fourier analysis of the radial component of the field on a cylinder of radius 6 mm, taking mode numbers up to 9 azimuthally, and 39 longitudinally. We then calculated the Cartesian coefficients using equation (3), with $k_x = 2\pi/192$ mm^{-1}. Figure 2 shows the residual of the fit to the vertical field component on the mid-plane, and on a plane 6 mm above the mid-plane. On the mid-plane, the residual is less than a Gauss everywhere; close to the field tip, the residual is a few tens of Gauss.

CALCULATING THE DYNAMICAL MAP

Having obtained a good fit of an analytical expression for the field to the numerical field data, a Differential Algebra (DA) code can be used to integrate the equations of motion in the field to produce a dynamical map in Taylor form. We have used the code COSY [5] for this; other differential algebra codes are available. COSY includes a 7th order Runge-Kutta integrator that solves the exact equations of motion for a relativistic particle in magnetic field. Because the integration is not explicitly symplectic, the result is a map that has (small) symplectic errors in some of the lower-order terms. For comparison, we have also implemented an explicit symplectic integrator [6] that solves Hamilton's equations with the small-angle approximation for the Hamiltonian.

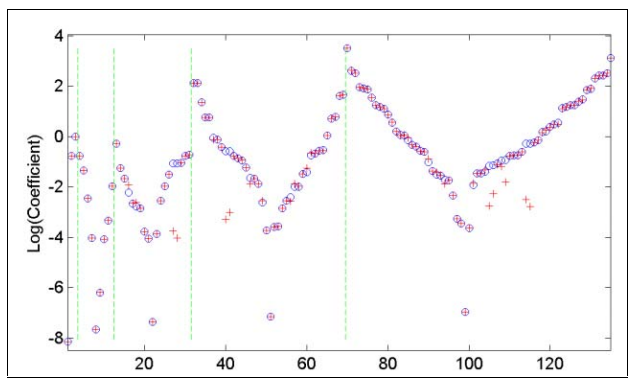

Figure 3: Coefficients in the 5th order map for x through one period of the BL11 wiggler, calculated with Runge-Kutta integration (blue points), and an explicit symplectic integrator (red crosses). Green lines divide terms of different order.

Figure 3 compares the coefficients of different terms in the map for x from the two integration methods for one period of the SPEAR2 BL11 wiggler. There are small differences between the maps, related to the small-angle approximation in the explicit symplectic integrator. Both integrators produce maps with small symplectic error.

TUNE SHIFTS FROM BL11 WIGGLER

After the BL11 wiggler was installed in SPEAR2, strong nonlinear effects were observed. Measurements were made of the tune shift with amplitude [2]. We used an interpolated Fourier-Hanning technique to determine

numerically the effect of the BL11 wiggler on the dynamics in a model of the SPEAR2 lattice, using the map produced using COSY. We found a linear horizontal tune shift of –0.010, in excellent agreement with the experimental observation of –0.009. We found a tune shift with amplitude of -4.5×10^{-5} mm^{-2}, smaller than the experimentally observed value of -7.4×10^{-5} mm^{-2}. However, studies based on numerical integration through a field model produced in TOSCA, also reported in [2] underestimated the tune shift by the same amount; it appears likely that the discrepancy is due to an error in the model of the magnet, rather than in the analysis. We note that the theoretical studies in [2] calculated only the dynamic octupole component, equivalent to a single term in the map. The techniques presented above give a complete model of the dynamics.

DYNAMICS IN THE MDR WIGGLER

The NLC MDR wiggler has a peak field of 2.1 T, a period of 270 mm, and a gap of 18 mm. A field map has been produced using TOSCA. Figure 4 shows the divergence and curl of the field, calculated on a horizontal plane 6 mm above the mid-plane. The deviation from the ideal value of zero has a similar pattern to the SPEAR2 BL11 wiggler, but is a little larger.

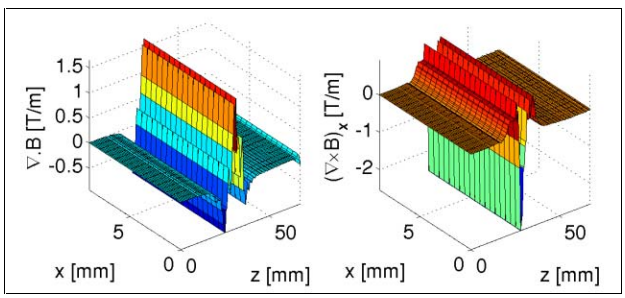

Figure 4: Field divergence and curl of the NLC MDR wiggler field map, 6 mm above the mid-plane.

Figure 5 shows residuals of the fit to the MDR wiggler, using the same procedure and same number of modes as for the SPEAR2 BL11 wiggler. The relatively large residuals on the mid-plane may be due to deviations from the constraints of Maxwell's equations.

Finally, Figure 6 shows the dynamic aperture in co-ordinate space and in tune space for the NLC MDR with a linear wiggler model, and with a 5th order map from the Runge-Kutta integration through the field in COSY. The colors of the points indicate the diffusion rate in tune space on a logarithmic scale. Particles were tracked for 512 turns. At the observation point, the injected rms beam size is 0.8 mm horizontally, and 0.25 mm vertically. The wiggler has some small impact on the tune shifts, but the nonlinear dynamics are dominated by the sextupoles. The results need to be confirmed using a more accurate field map.

The off-energy dynamics in the lattice remain a concern, with little margin for the 1% full-width energy spread on the incoming beam.

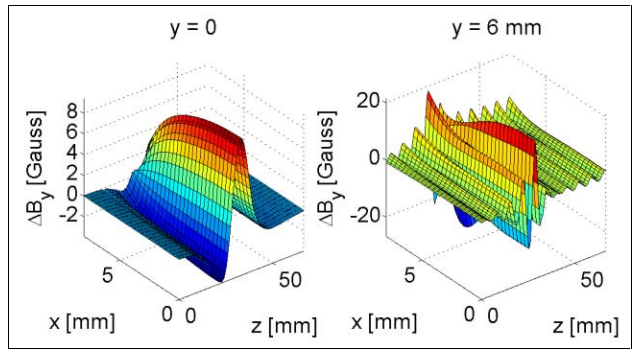

Figure 5: Residual of a fit to the NLC MDR wiggler field map.

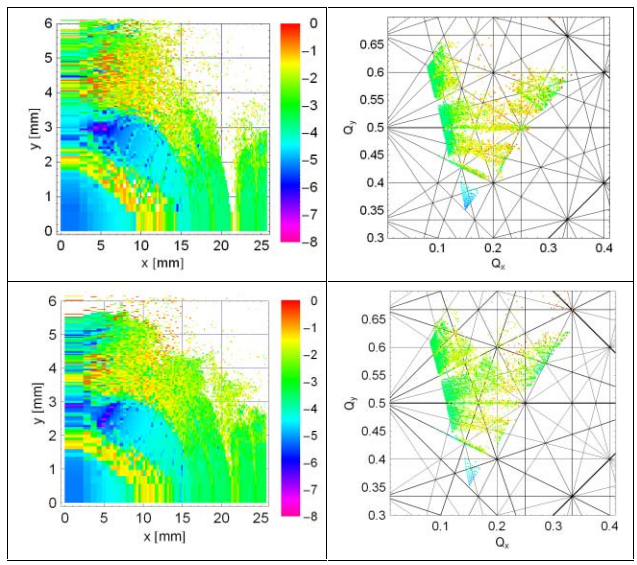

Figure 6: Dynamic aperture and frequency map for the NLC MDR with linear wiggler model (top) and 5th order map for each wiggler period (bottom).

ACKNOWLEDGEMENTS

Many thanks to W. Wan (LBNL) for assistance with COSY. The Taylor maps for the NLC wiggler were also calculated by J.-F. Ostiguy using the DA code mxzyptlk.

REFERENCES

[1] A. Wolski, T.O. Raubenheimer, M.D. Woodley and J. Wu, "A Lattice with Larger Momentum Compaction for the NLC MDR," Proceedings, PAC 2003.

[2] J. Safranek et al, "Nonlinear Dynamics in a SPEAR Wiggler," Phys.Rev. STAB **5**, 010701 (2002).

[3] M. Venturini, A.Wolski and A. Dragt "Wigglers and Single-Particle Dynamics in the NLC Damping Rings," Proceedings, PAC 2003.

[4] O. Chubar, P. Elleaume, J. Chavanne, http://www.esrf.fr/machine/groups/insertion_devices/Codes/Radia/Radia.html

[5] M. Berz, http://cosy.pa.msu.edu/

[6] Y.K. Wu, E. Forest, D.S. Robin, Phys. Rev. E **68**, 046502 (2003).